



COBEM
2021 25th International Congress
of Mechanical Engineering



COB-2021-2234

AN ELASTIC METAMATERIAL BEAM LEVERAGING UNEVENLY TUNED LOCALLY RESONATING SYSTEMS FOR VIBRATION ATTENUATION

Renan Trevizan de Melo

Universidade Estadual Paulista “Júlio de Mesquita Filho” (Unesp) – Campus of São João da Boa Vista, São João da Boa Vista, SP
13876-750, Brazil
renan.trevizan@unesp.br

Carlos De Marqui Junior

University of São Paulo (USP) – Department of Aeronautical Engineering, Engineering School of São Carlos, São Carlos, SP
13566-590, Brazil
demarqui@sc.usp.br

Vagner Candido de Sousa

Universidade Estadual Paulista “Júlio de Mesquita Filho” (Unesp) – Campus of São João da Boa Vista, São João da Boa Vista, SP
13876-750, Brazil
vagner.sousa@unesp.br

Abstract: *This research presents an analysis about elastic metamaterials with unevenly tuned locally resonant systems, in an effort to promote vibration attenuation with no addition of extra mass to the host structure. For this purpose, the equations of motion for a five-resonator metamaterial beam under harmonic base excitation were solved in frequency domain for a range of excitation frequencies. Transmissibility plots were obtained so that a number of different case studies could be compared with a reference case (uniform configuration). The most attractive case studies show that when certain resonators (identified here as #3 and #5) have their masses decreased by 30% the bandgap bandwidth increases by 21.95%. Moreover, when an expressive mass reduction of 41% in resonator #4 was also considered, the bandgap increased by 35%. Additional modifications on the resonators #1 and #2 promoted improvements of 85.45% on the bandgap bandwidth when their target frequencies have been decreased by 36% and 19%, respectively (achieved by decreasing the corresponding spring stiffness). Therefore, we may conclude that carefully tuned non-uniform resonators can significantly improve the model response (in terms of bandgap bandwidth) and reduce the mass added by the resonators.*

Keywords: *elastic metamaterials, resonant systems, vibrations, transmissibility, bandgap bandwidth.*

1. INTRODUCTION

Mechanical vibrations represent one of the main factors related to the early fatigue of materials. Several traditional techniques are used in vibrational control, and the adjustment of the mass, stiffness and damping parameters of a system allows, in many cases, the control of its behavior when subjected to some type of harmonic excitation, avoiding the occurrence of more severe vibrations for operation at frequencies close to resonances (Meirovitch, 1997). Modern techniques related to vibration control tend to involve the use of the so-called intelligent materials (or smart materials), studied more expressively in the past few years by authors like Giurgiutiu (2000), Erturk and Inman (2008), Barzegari *et al.* (2015) and Shivashankar and Gopalakrishnan (2020).

Metamaterials (Liu *et al.*, 2000) are also the target of new research (Nimmagadda *et al.*, 2019) in vibration control (Sugino *et al.*, 2016, 2017), sound absorption (Liao *et al.*, 2019), wave guiding or trapping, energy harvesting (Alshaqqa and Erturk, 2021), among other applications. Metamaterials can be combined in advanced configurations, further optimizing the results, or adding new functionalities to the system such as the ability to exchange energy between different physical domains (Sousa *et al.*, 2018a, 2018b; Sugino *et al.*, 2020; Alshaqqa and Erturk, 2021).

Metamaterials, in particular, can be obtained using different types of resonator elements in an optimized way (not necessarily based on intelligent materials), and are designed to exhibit characteristics not normally found in a natural way. One of the characteristics that can be obtained with a metamaterial is the formation of a bandgap, that is, a region of attenuation of vibrations around a range of excitation frequencies, which can comprise low frequencies even in relatively small structures (Sugino *et al.*, 2016, 2017).

The first analyzes about the formation of the bandgap involved acoustic metamaterials, and were presented by Liu *et al.* (2000), bringing new perspectives for research in the area. From a mechanical point of view, Yu *et al.* (2006)

innovated by investigating a flexural bandgap, based on an Euler-Bernoulli beam with vibration absorbers of two degrees of freedom. For this purpose, it used a transfer matrix approach to determine the expected response, which was validated by means of finite element modeling with experimental tests.

Sugino *et al.* (2016) proposed to evaluate a case pertinent to finite structures, whose dynamic response is determined by the modal forms of the structure. In this way, it employed a modal analysis approach for the formation of the bandgap in locally resonant metamaterials for a uniform case. The studies promoted in this case validated the assumption of infinite absorbers in a finite structure, allowing the allocation of the bandgap in a desired frequency range.

Sousa *et al.* (2018a, 2018b) took up to the problem of locally resonant metamaterials again with the use of intelligent materials (shape memory alloys in particular). Acoustic/elastic metamaterials made from purely mechanical resonant components generally do not exhibit reconfigurable and adaptive characteristics, since the bandgap frequencies depend on the mass ratio of the structure (*i.e.*, the total mass added by the resonators to the mass of the plain host structure). In this context, the replacement of conventional, inactive resonators with resonators consisting of shape memory alloy (SMA) elements brings an improved tuning behavior, making the properties of the bandgap adjustable in view of the change in the elastic modulus of SMAs with temperature as its crystallographic lattice changes between martensite and austenite.

The aforementioned cases contributed to the understanding of the behavior and applicability of metamaterials in the control of vibrations, demonstrating the possibility of allocating and tuning the bandgap in a convenient way. These studies, however, started from uniform configurations for the resonators distributed throughout the metamaterial. In view of this, this work conducts an investigation about the effects of non-uniform tuning of locally resonant systems on the dynamic structural response of a metamaterial. The main goal is to increase the bandgap bandwidth without the need of significant increases in mass.

2. MODAL ANALYSIS OF A BANDGAP FORMATION

Consider an uniform Euler-Bernoulli beam, with arbitrary boundary conditions, flexural stiffness EI , linear density of mass m , and length L (Figure 1). Added to this, a transverse base excitation $w_b(t)$, with relative transverse vibrations denoted by $w(x, t)$ and absolute displacement $w_{abs}(x, t) = w_b(t) + w(x, t)$. It is assumed that the system is undamped since modal damping may be included later. The allocation of S absorbers (undamped spring mass systems) is considered attached to the beam in positions x_j , with masses m_j , stiffness k_j , squared natural frequencies $\omega_{aj}^2 = k_j/m_j$, and relative displacements u_j , for $j = 1, 2, \dots, S$.

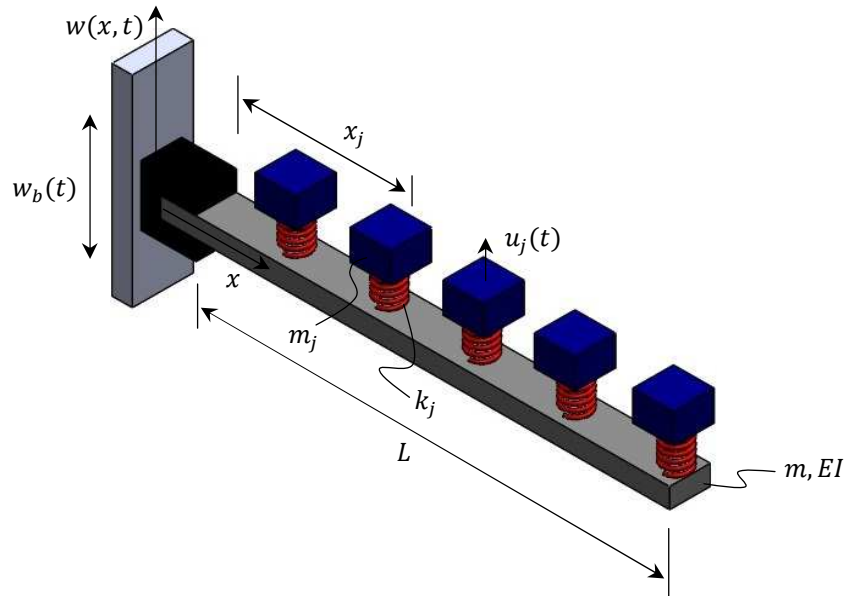


Figure 1. Schematic of a metamaterial, in this case, a cantilever beam under base excitation with purely mechanical resonators.

The equation of motion for the beam in physical coordinates, in the absence of external forces, is given by

$$EI \frac{\partial^4 w}{\partial x^4} + m \frac{\partial^2 w}{\partial t^2} - \sum_{j=1}^S m_j \omega_{aj}^2 u_j(t) \delta(x - x_j) = -m \ddot{w}_b(t), \#(1)$$

where $\delta(x)$ is the Dirac delta function (Sugino *et al.*, 2016). In this case, the equation for each resonator takes the form

$$\ddot{u}_j(t) + \omega_{aj}^2 u_j(t) + \frac{\partial^2 w}{\partial t^2}(x_j, t) = -\ddot{w}_b(t). \#(2)$$

The natural frequencies ω_i and the vibration modes $\phi_i(x)$ are known (Paz and Kim, 2019) for the beam in the absence of resonators, and are denoted by

$$\omega_i = (\beta_i L)^2 \sqrt{\frac{EI}{mL^4}}, \#(3)$$

and,

$$\phi_i(x) = A_i \left[(\cosh \beta_i x - \cos \beta_i x) + \left(\frac{\cos \beta_i L + \cosh \beta_i L}{\sin \beta_i L + \sinh \beta_i L} \right) (\sinh \beta_i x - \sin \beta_i x) \right], \#(4)$$

where $\beta_i L$ represents the eigenvalues of the problem, which are obtained from the characteristic equation for a cantilever beam (with clamped-free boundary conditions),

$$\cos \beta L \cosh \beta L = -1. \#(5)$$

In addition, the modes of vibration are normalized, so that the following equality is valid,

$$\int_0^L \phi_i(x) \phi_j(x) dx = L \delta_{ij}, \#(6)$$

where δ_{ij} is the Kronecker Delta.

The transverse displacements of the beam can be obtained by

$$w(x, t) = \sum_{k=1}^N \phi_k(x) \eta_k(t), \#(7)$$

where N is the number of modes considered.

The substitution of Eq. (7) into Eqs. (1) and (2), applying the conditions of orthogonality (Meirovitch, 1997), allows expressing the governing equations in modal coordinates (Sugino *et al.*, 2016) as

$$\sum_{i=1}^N \left[\delta_{ik} + \sum_{j=1}^S \hat{m}_j \phi_i(x_j) \phi_k(x_j) \right] \ddot{\eta}_i(t) + \sum_{j=1}^S \hat{m}_j \phi_k(x_j) \ddot{u}_j(t) + \omega_k^2 \eta_k(t) = -\ddot{w}_b(t) \left(\int_0^L \phi_k(x) dx + \sum_{j=1}^S \hat{m}_j \phi_k(x_j) \right), \#(8)$$

and,

$$\ddot{u}_j(t) + \omega_{aj}^2 u_j(t) + \sum_{i=1}^N \ddot{\eta}_i(t) \phi_i(x_j) = -\ddot{w}_b(t), \#(9)$$

where $\hat{m}_j = m_j/(mL)$ corresponds to the normalized mass of the j -th resonator, assuming that the free indices k and j go from 1 to N and from 1 to S , respectively.

In this way, Eqs. (8) and (9) constitute a system with $N + S$ coupled second order differential equations, whose solution can be obtained in different ways. The index i denotes the coupling between the modes, and goes from 1 to N .

In particular, the approximate resonant frequencies and modal shapes of the entire structure can be obtained through an eigenvalue problem, the solution of which can be done in a numerical way both for time domain, considering the above equations, and in the frequency domain, based on the amplitudes of interest oscillations. Assuming harmonic

oscillations for a given excitation frequency ω , and using an over bar to indicate amplitude terms, Eq. (9) can be solved for the amplitude of the resonators (Sugino *et al.*, 2016),

$$\bar{u}_j = \frac{\omega^2}{\omega_{aj}^2 - \omega^2} \sum_{i=1}^N \bar{\eta}_i \phi_i(x_j) + \frac{\omega^2}{\omega_{aj}^2 - \omega^2} \bar{w}_b. \#(10)$$

Finally, by replacing Eq. (10) into Eq. (8), we obtain a generalized formulation for determining the amplitudes ($\bar{\eta}$), concerning the modal displacements, which allows a treatment of the problem in the frequency domain to visualize the formed bandgap due to the allocation of the tuned resonators based on an objective frequency ω_t , not restricted to any type of uniformity according to this model equation. The final expression of interest therefore takes the form

$$(\omega_k^2 - \omega^2) \bar{\eta}_k - \omega^2 \sum_{i=1}^N \sum_{j=1}^S \frac{\hat{m}_j \omega_{aj}^2}{\omega_{aj}^2 - \omega^2} \phi_i(x_j) \phi_k(x_j) \bar{\eta}_i = \bar{Q}_k, \#(11)$$

where,

$$\bar{Q}_k = \bar{w}_b \omega^2 \left(\frac{1}{L} \int_0^L \phi_k(x) dx + \sum_{j=1}^S \frac{\hat{m}_j \omega^2}{\omega_{aj}^2 - \omega^2} \phi_k(x_j) \right). \#(12)$$

3. CASE STUDIES AND RESULTS

Equations (11) and (12) were solved numerically in the frequency domain by means of a matrix equation. For the purposes of simulation, the first 15 shape modes of the beam ($N = 15$), and five resonators ($S = 5$), were considered, these numbered from #1 to #5 from the base to the tip of the beam.

The data that comprised the structured algorithm included the geometric and structural parameters of the main beam and the resonators. The beam comprises an aluminum piece with a length (L) of 0.2 m, mass per unit length (m) equal to 0.3256 kg/m and flexural stiffness (EI) of 0.45258 N.m². The resonators, in turn, initially comprise five resonant beams with masses (m_{aj}) equal to 0.00911 kg and are evenly distributed along the main beam. The natural frequencies (and, therefore, their target frequencies) were chosen so that $\omega_{aj} = \omega_t = 0.868\omega_2$.

3.1 Parametric analysis

A parametric analysis was carried out fixing, at first, the resonators stiffness in order to verify the effect brought about by the exclusive modification of the masses. Initially individually and later jointly.

The reduction in the masses of resonators #1 and #2 deconstructed the original bandgap, maintaining a potentially unwanted resonance peak. This reduction for resonators #3 and #5, however, did not deconstructed the original bandgap, and brought noticeable additions to its extension. Reducing the mass of resonator #4, still in an isolated manner, mischaracterized the bandgap, but generated a significant increase in its extension. Furthermore, increases of more than 30% in the frequency of the resonators evaluated one by one, did not present positive contributions to the bandgap.

In view of the predicted behavior, the universe of choices associated with joint modifications of the resonators was restricted, and simulations were performed for different configurations. Among these, the five most attractive cases were selected and evaluated. For the initial four cases, the focus of the modifications was to reduce between 10% and 30% the masses of resonators listed from #3 to #5. In a second step, tests contemplating the reduction in the frequency of resonators #1 and #2 (obtained in terms of the increase in stiffness) were performed, and the best configuration was selected. Table 1 describes the parameters that characterize the best cases observed.

Table 1. Characteristic parameters referring to the most promising cases obtained.

Description	ω_{a1}	ω_{a2}	ω_{a3}	ω_{a4}	ω_{a5}	Σm_{aj}
Reference case	ω_t	ω_t	ω_t	ω_t	ω_t	0.0456kg
Case 1	ω_t	ω_t	$1.1\omega_t$	ω_t	$1.1\omega_t$	0.0424kg
Case 2	ω_t	ω_t	$1.1\omega_t$	ω_t	$1.2\omega_t$	0.0412kg
Case 3	ω_t	ω_t	$1.2\omega_t$	ω_t	$1.2\omega_t$	0.0400kg
Case 4	ω_t	ω_t	$1.1\omega_t$	$1.3\omega_t$	$1.2\omega_t$	0.0375kg
Case 5	$0.8\omega_t$	$0.9\omega_t$	$1.1\omega_t$	$1.3\omega_t$	$1.2\omega_t$	0.0375kg

3.2 Bandgap bandwidth and metamaterial beam transverse displacement

This section presents the results obtained through a more careful assessment of the cases previously described. The frequency distribution shown in Table 1 was followed by reducing the masses of the corresponding resonators (and increasing the stiffness of resonators #1 and #2, for case 5).

The transmissibility plots for the uniform case and other configurations of interest are shown in Figure 2. The predicted transmissibility for the plain beam is shown in the first plot (top-left) in red. The reference case (beam with uniform resonators tuned such that the bandgap is centered at the second beam resonance) is shown in blue. The reference case is also displayed in all other plots for comparison with the non-uniform cases. Transmissibility plots for the five cases presented in Table 1 are shown in Figure 2, following the order in that they appear in Table 1.

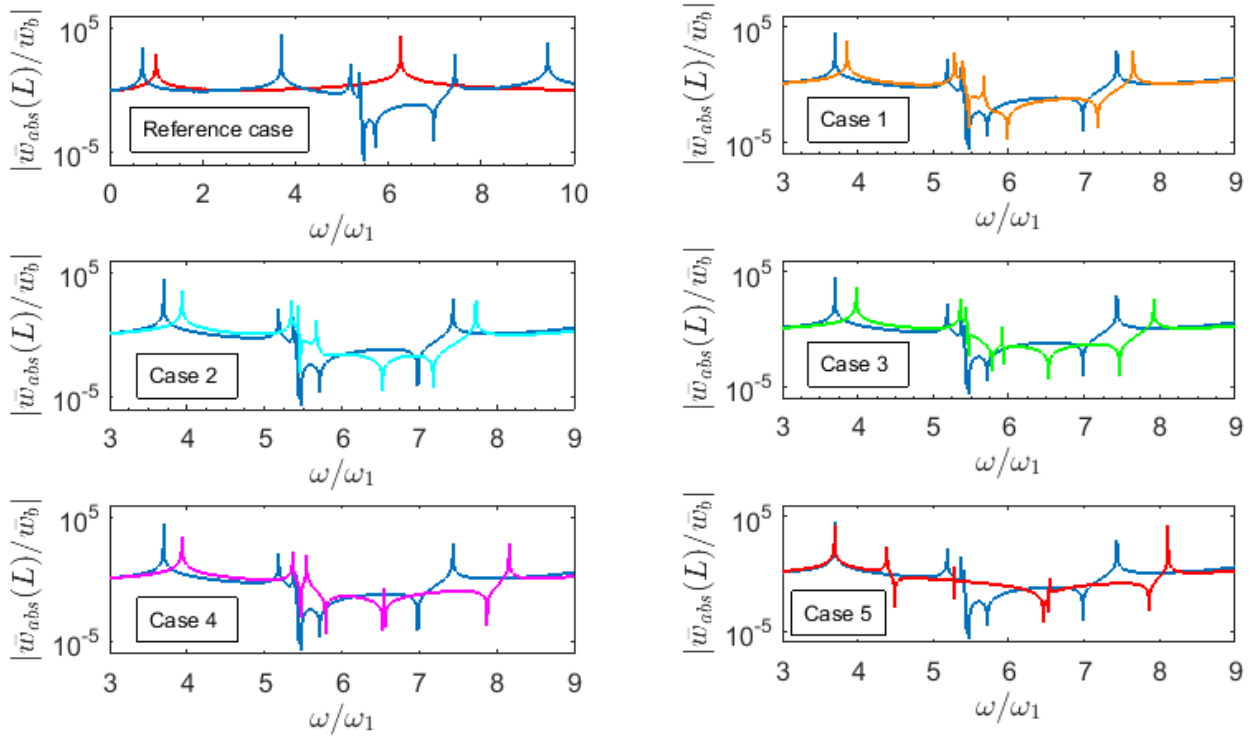


Figure 2. Transmissibility plots for the different cases considered in this study. In the first plot (top-left), the transmissibility of the plain beam is shown in red, while the reference case (beam with uniform resonators) is shown in blue. The reference case is displayed in all of the plots for comparison with the non-uniform cases.

As shown in Figure 2, the non-uniform cases exhibit increasing extensions in the total bandgap bandwidth when compared with the reference case. This increase was measured based on the range between the resonant frequencies that are located at the edges of the bandgap. As a result, there are increases from 9.12% to 85.45%, as identified in Table 2.

Table 2. Increases of bandgap bandwidth.

Description	Bandgap increase
Case 1	9.12%
Case 2	11.75%
Case 3	21.92%
Case 4	34.81%
Case 5	85.45%

Although bandgap bandwidth increases are predicted, defects are clearly introduced in the form of energy localization. Based on the theory (Sugino *et al.*, 2016, 2017), no system eigenvalues fall within the bandgap boundaries in the reference (uniform) case. On the other hand, some eigenvalues may appear inside the bandgap in the non-uniform cases, yielding undesired resonances within the bandgap boundaries. Such resonances are a side effect of the uneven tuning of the resonators and are currently a topic of study. Damping augmentation, for example, may be pointed out as

an workaround for such an issue. The combination with other techniques (such as the adaptive resonant shunt circuits presented in Silva *et al.*, 2020) may also be a possibility for response enhancements.

For a better visualization of the studied effect, some frequencies of interest were selected (namely, ω/ω_1 equal to 4.00, 4.65, 5.37, 6.50, 7.80 and 9.30), for which the behavior of the metamaterial was plotted. In the first instance, the effect brought about on the relative displacement of the beam tip is more noticeable for frequencies above the upper edge of the reference bandgap. The latter now has smaller amplitude of oscillation for the modified configurations, especially for the cases that present more significant amplifications of the bandgap. In addition, the vibration of the metamaterial as a whole is affected by the distribution of the resonators, so that the attenuation effect can be observed along the entire length of the main beam. The resonators act oscillating in phase with the beam for frequencies below the target frequency, and in opposition of phase for higher frequencies, having their amplitude of oscillation directly linked to the chosen tuning frequency and the frequency of interest evaluated. Figure 3 illustrates the beam shape and the displacement of the resonators in each case for the considered frequencies.

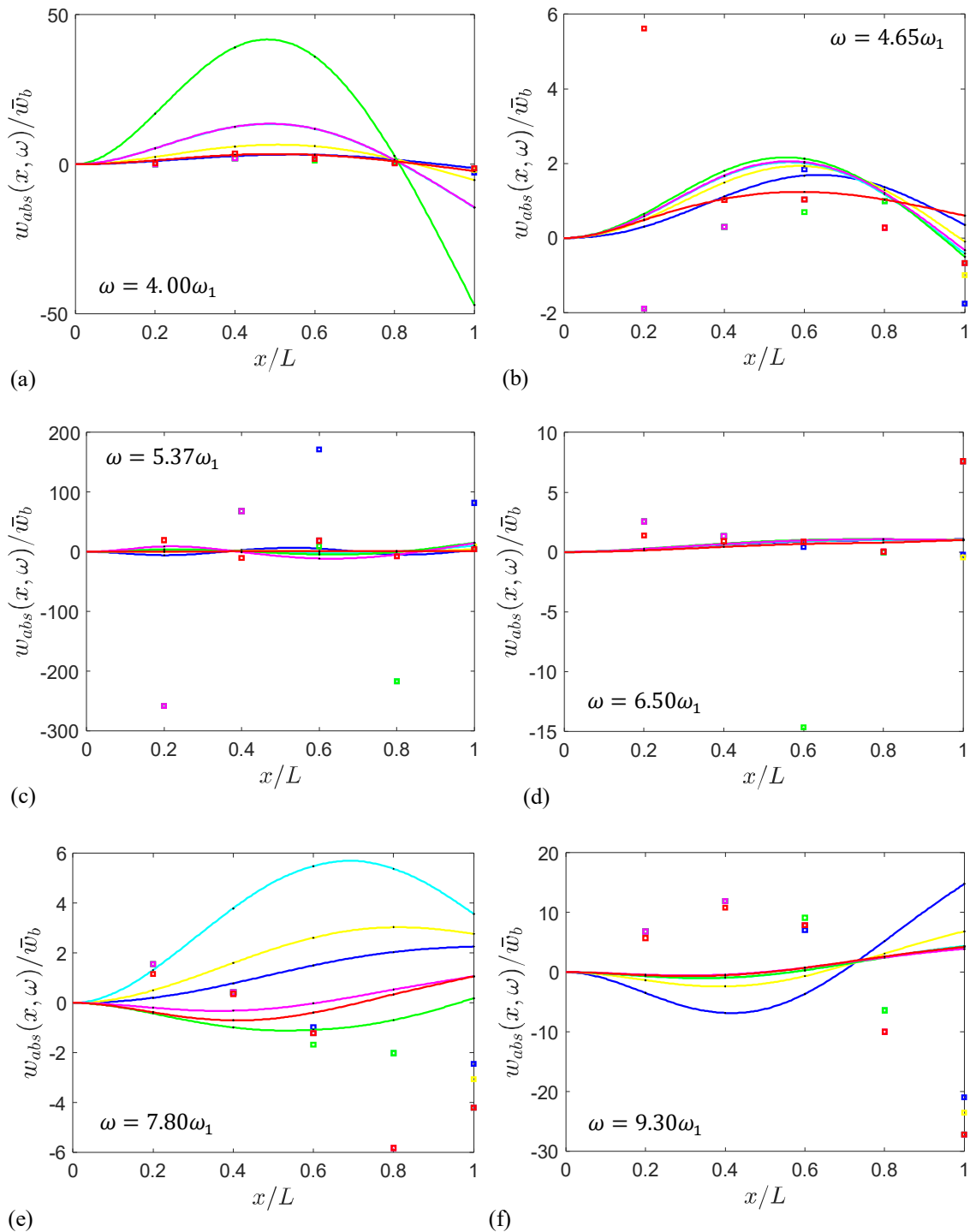


Figure 3. Transverse displacements of the metamaterial for the uniform case (blue) and other configurations of interest (case 1: yellow; case 2: cyan; case 3: green; case 4: magenta; case 5: red) to the selected frequency given by the values of ω/ω_1 equal to 4.00, 4.65, 5.37, 6.50, 7.80 and 9.30, respectively.

The displacement of the metamaterial is shown along the length of the beam for the selected frequencies, as well as the amplitude of oscillation of the resonators, which is maximum at the target frequency (Figure 3 (c)). For excitation frequencies located inside the bandgaps (Figures 3(c) and 3(d)), the response of the metamaterial is only slightly modified, maintaining a very close attenuation level for all cases. The other bands allow visualizing an overall attenuation effect more optimized for case 5 at frequencies lower than the target frequency (Figures 3(a) and 3(b)), since this is the only case that extends the bandgap to left, and for cases 4 and 5 at frequencies higher than this (Figures 3(e) and 3(f)).

4. CONCLUSIONS

In this work, we studied an elastic metamaterial with unevenly tuned locally resonating systems, in an effort to improve vibration attenuation with no addition of extra mass (with respect to the uniform configuration). An analytical model for a locally resonant metamaterial beam in transverse vibrations was considered, and equations of motion for a five-resonator metamaterial beam under harmonic base excitation were solved in frequency domain for a range of excitation frequencies.

Transmissibility plots (a measure of mechanical input-output relationship) were obtained and a number of different case studies could be compared. A reference case was obtained for resonators evenly tuned at the same natural frequency (which also correspond to the metamaterial target frequency), and numerical predictions showed that when certain resonators (hereby identified as #3 and #5) have their masses decreased by 30%, the bandgap bandwidth increases by 22% (when compared with the reference case). Moreover, when an expressive mass reduction of 41% in resonator #4 was also considered, the bandgap increased by 35%. On the other hand, resonators #1 and #2 promoted improvements of 85% on the bandgap bandwidth when their natural frequencies (and, therefore, their target frequencies) also decreased by 36% and 19%, respectively (achieved by decreasing the corresponding spring stiffness). We may conclude, therefore, that carefully tuned non-uniform resonators can significantly improve the model response (in terms of bandgap bandwidth). Moreover, in a number of cases the proper tuning of the resonators also helps in decreasing the mass added by the resonators.

5. ACKNOWLEDGEMENTS

This work was supported by the São Paulo Research Foundation (FAPESP) [Grant numbers 2019/25680-0 and 2018/15894-0].

6. REFERENCES

- Alshaqqaq, M. and Erturk, A., 2020. "Graded multifunctional piezoelectric metastructures for wideband vibration attenuation and energy harvesting". *Smart Materials and Structures*, Vol. 30, No. 1, p. 015029.
- Bachmann, F., Oliveira, R., Sigg, A., Schnyder, V., Delpero, T., Jaehne, R., Bergamini, A., Michaud, V., and Ermanni, P., 2012. "Passive damping of composite blades using embedded piezoelectric modules or shape memory alloys wires: a comparative study". *Smart Materials and Structures*, Vol. 21, No. 7, p. 075027.
- Erturk, A. and Inman, D.J., 2008. "A Distributed Parameter Electromechanical Model for Cantilevered Piezoelectric Energy Harvesters". *Journal of Vibration and Acoustics*, Vol. 130, No. 4, p. 041002.
- Giurgiutiu, V., 2000. "Review of Smart-Materials Actuation Solutions for Aeroelastic and Vibration Control". *Journal of Intelligent Material Systems and Structures*, Vol. 11, No. 7, pp. 525–544.
- Liao, Y., Zhou, X., Chen, Y and Huang, G., 2018. "Adaptive metamaterials for broadband sound absorption at low frequencies". *Smart Materials and Structures*, Vol. 28, No. 12, p. 025005.
- Liu, Z., Zhang, X., Mao, Y., Zhu, Y.Y., Yang, Z., Chan, C.T. and Sheng, P., 2000. "Locally Resonant Sonic Materials". *Science*, Vol. 289, No. 5485, pp. 1734–1736.
- Meirovitch, L., 1997. "Principles and Techniques of Vibrations". Prentice-Hall, Inc., Upper Saddle River, NJ.
- Nimmagadda, C. and Matlack, K. H., 2019. "Thermal tunable bandgaps in architected metamaterial structures". *Journal of Sound and Vibration*, Vol. 439, pp. 29–42.
- Paz, M. and Kim, Y. H., 2019. "Structural Dynamics", 6th ed. Springer Nature Switzerland AG.
- Shivashankar, P. and Gopalakrishnan, S., 2020. "Review on the use of piezoelectric materials for active vibration, noise, and flow control". *Smart Materials and Structures*, Vol. 29, No. 5, p. 053001.

- Silva, T.M.P., Clementino, M.A., Sousa, V.C. and De Marqui Junior, C., 2020. "An Experimental Study of a Piezoelectric Metastructure With Adaptive Resonant Shunt Circuits". *IEEE-ASME Transactions on Mechatronics*, Vol. 25, No. 2, pp. 1076–1083.
- Sousa, V.C., Sugino, C., De Marqui Junior, C. and Erturk, A., 2018a. "Adaptive locally resonant metamaterials leveraging shape memory alloys". *Journal of Applied Physics*, Vol. 124, p. 064505.
- Sousa, V.C., Tan, D., De Marqui Junior, C., and Erturk, A., 2018b. "Tunable metamaterial beam with shape memory alloy resonators: Theory and experiment". *Applied Physics Letters*, Vol. 113, p. 143502.
- Sugino, C., Leadenham, S., Ruzzene, M., and Erturk, A., 2016. "On the mechanism of bandgap formation in locally resonant finite elastic metamaterials". *Journal of Applied Physics*, Vol. 120, p. 134501.
- Sugino, C., Ruzzene, M. and Erturk A., 2020. "An analytical framework for locally resonant piezoelectric metamaterial plates". *International Journal of Solids and Structures*. Vol. 182–183, pp. 281–294.
- Sugino, C., Xia, Y., Leadenham, S., Ruzzene, M., and Erturk, A., 2017. "A general theory for bandgap estimation in locally resonant metastructures". *Journal of Sound and Vibration*, Vol. 406, pp. 104–123.
- Yu, D., Liu, Y., Zhao, H., Wang, G., and Qiu, J., 2006. "Flexural vibration band gaps in Euler-Bernoulli beams with locally resonant structures with two degrees of freedom". *Physical Review B*, Vol. 73, No. 6, p. 064301.

7. RESPONSIBILITY NOTICE

The authors are the only responsible for the printed material included in this paper.